



Research Article

Determination of Lying Posture through Recognition of Multitier Body Parts

Tae-Hwan Kim, Soon-Ju Kwon, Hyun-Min Choi, and Youn-Sik Hong

Department of Computer Science and Engineering, Incheon National University, Incheon, 406-772, Republic of Korea

Correspondence should be addressed to Youn-Sik Hong; yshong@inu.ac.kr

Received 25 December 2018; Revised 27 February 2019; Accepted 20 March 2019; Published 8 April 2019

Academic Editor: Giancarlo Fortino

Copyright © 2019 Tae-Hwan Kim et al. This is an open access article distributed under the Creative Commons Attribution License, which permits unrestricted use, distribution, and reproduction in any medium, provided the original work is properly cited.

In this paper, we propose a lying posture discrimination algorithm to monitor the behavior pattern of a person lying in bed. Using FSR (force sensing resistor) sensors arranged in a grid structure, three major body parts such as *head*, *shoulder*, and *hips* are identified, and six lying positions are determined based on these body parts. Head, shoulder, and hips are relatively high in pressure and are easy to distinguish due to low movement. In addition, we have effectively limited the search space to identify the above body parts based on standard body dimensions. Experimental results show that there is a correlation between pressure distribution and lying posture. The results of this study can be applied to the monitoring of sleep posture and can also be used as an aid to prevent fall accidents and the occurrence of pressure ulcers of elderly patients who are unable to move.

1. Introduction

Currently, Korea has entered an aged society in 2018 and the number of nursing hospitals for the care of the elderly is increasing rapidly [1]. However, 18.2% of the elderly patients are reported to experience falls each year at such nursing hospitals [2–5]. In addition, there is a high possibility of a pressure ulcer in an elderly patient who cannot move himself or herself. A pressure ulcer is the symptom of a mixture of body load and friction that causes local damage to the skin tissue at the protrusion of the bone [6]. In elderly patients who cannot move by themselves, caregivers should change their postures at least once every 90 minutes to prevent pressure ulcers [6, 7]. Elderly care hospitals are growing rapidly, but there is an absolute shortage of nursing staff. If this lack of nursing staff prevents the elderly from taking proper care of them, it is likely that the condition of the elderly patients will become worse due to falls and pressure ulcers.

Besides, human's sleeping pose can have a major impact on his/her slumber as well as his/her overall health. The disorder sleep patterns can cause many diseases. The purpose of this study is to analyze sleep behavior pattern by monitoring the posture of a person lying in bed in real time. It also determines how the elderly patient who cannot move himself or herself behaves in bed. It is aimed to increase nursing

efficiency by informing the nursing staff in advance of the risk of falling and the possibility of pressure ulcer occurrence.

To this end, in this paper, we propose a method of arranging pressure sensors in a grid structure to discriminate the human's lying position regardless of physical conditions. We also present a multitier algorithm to effectively discriminate the lying posture. *Tier-1* is defined as a region where the pressure in the body part is high and it is continuously maintained due to the low frequency of movement. The body parts belonging to the tier-1 are *head*, *shoulder*, and *hips*. In some typical lying postures, these body parts maintain a straight line. Based on this, it is possible to distinguish whether a person is lying in the upright posture (Figure 2(b)), the left posture (Figure 2(a)), or the right posture (Figure 2(c)).

There are many postures in bed: lying on either side, with the body straight or bent/curled forward or backward. The key idea of the method to be proposed here is to determine the lying posture based on the upper body. In general, the weight of an upper body of a person is equivalent to 75% of the body weight [8]. In addition, the combined weight of the head, shoulders, and hips belonging to the tier-1 is 48% of the body weight [8]. In other words, it is advantageous to discriminate based on the upper body when recognizing the lying postures using the pressures sensed. For example, suppose that a person is lying in the upright posture, and we found the

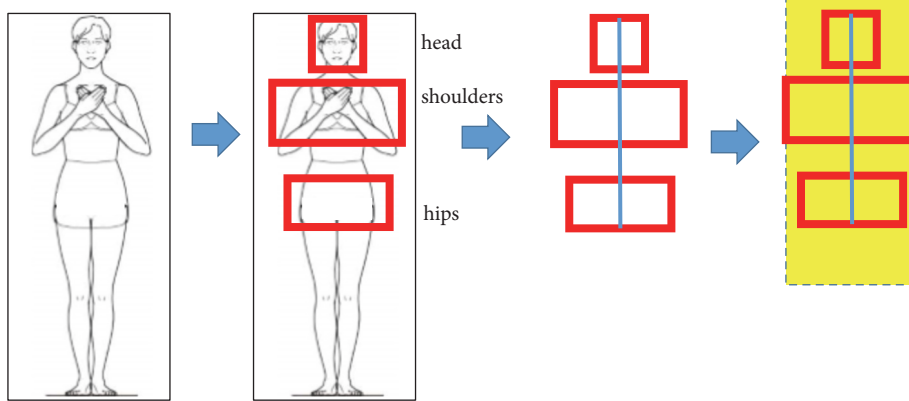


FIGURE 1: A process of discriminating lying posture based on the body parts belonging to the tier-1.

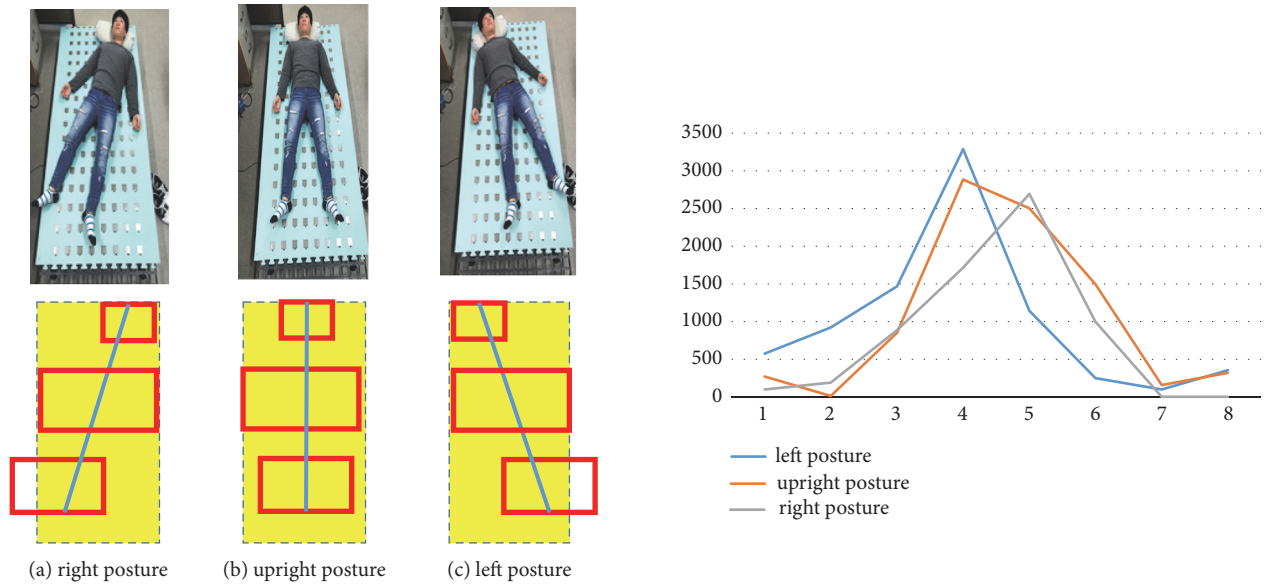


FIGURE 2: A determination of 3 basic lying postures and the corresponding distribution curves.

body parts belonging to the tier-1 as shown in Figure 1. To determine the lying posture, the area corresponding to the shoulder can be extended in both the vertical directions. Then we can check whether the extended area includes both the head and the hips.

Based on the above criteria, the basic three postures, *upright*, *left*, and *right* posture, as shown in Figure 2 can be easily identified. The pressure distribution curves for them as shown in the right of Figure 2 are very similar because the cumulative sum of the pressure values of each posture is almost the same. In the pressure distribution curve, the number in the x-axis corresponds to the column in the grid structure. Also, the value of the y-axis represents the cumulative sum of the pressure values which belong to the corresponding column. Notice that the pressure distribution is the sample measured at time t .

In order to determine the other lying postures rather than the basic postures, it is necessary to analyze the pressure distribution. As shown in Figure 3, when a person lies

in a bent posture, the curve of the pressure distribution is somewhat different from those of the basic postures in Figure 2. Also, when lying down in a bent posture, the cumulative sum of the pressure values decreases because the area under pressure is reduced compared to the basic postures.

Unlike the body parts belonging to the tier-1, hands, feet, etc. have relatively low pressure but high frequency of movement [9]. There is a possibility that the body parts corresponding to the tier-2 or tier-3 may not be found when the pressure value is sampled at a predetermined time interval. Therefore, it is more effective in determining the bent posture based on the pressure distribution.

In this paper, we propose an algorithm to discriminate six lying postures including prone posture based on the tier-1 model. The contribution of the method to be presented is that it uses only three major parts of the upper body to determine the lying position. The pressure distribution is also considered to improve the accuracy of lying posture determination.

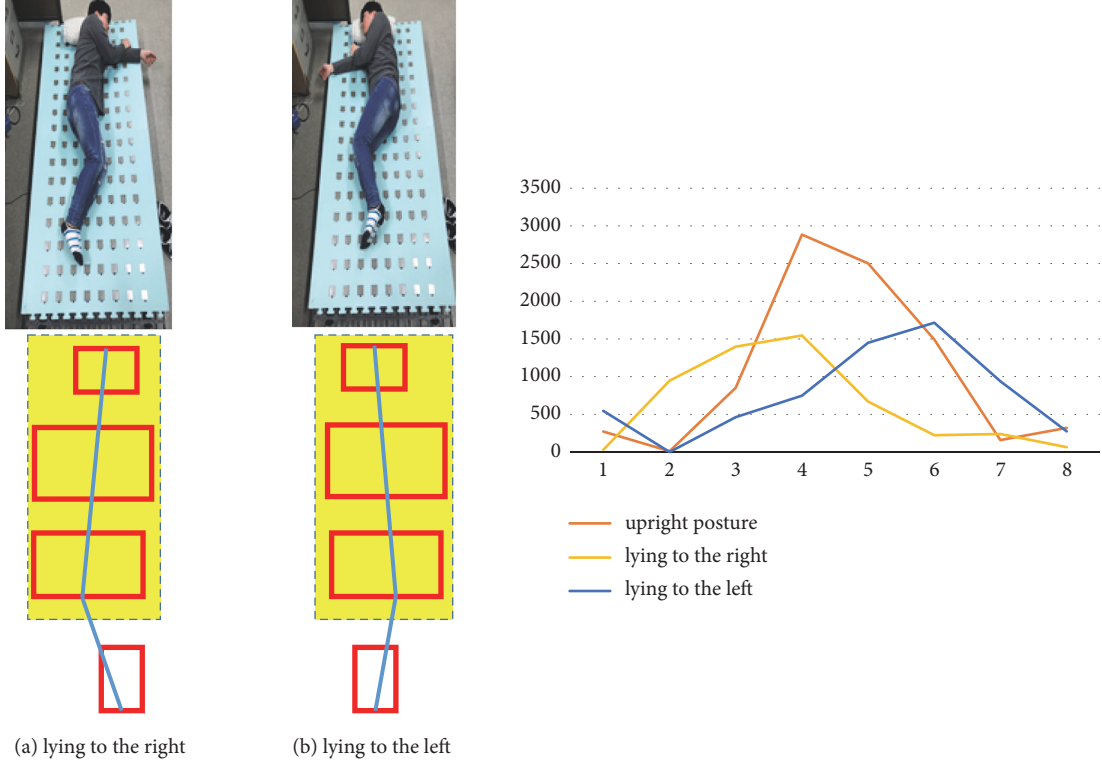


FIGURE 3: A determination of 3 basic lying postures and the corresponding distribution curves.

Even though only a limited number of pressure sensors are used instead of the sensor arrays, the accuracy of the proposed method is 90% when determining the lying posture using five consecutive pressure distributions. The algorithm proposed in this paper can be used to monitor the sleeping posture of elderly as well as ordinary people.

The remainder of this paper is organized as follows. Section 2 summarizes related works. In Section 3, we explain the system configuration. Section 4 describes multilayer based lying posture discrimination algorithms, and Section 5 presents experimental results. In Section 6, conclusions are presented.

2. Related Works

A wireless body sensor network (BSN) is a particular type of WSN (wireless sensor network) applied to human body monitoring [10, 11]. Key benefit of this technology is the possibility of monitoring vital and physiological signs continuously and noninvasively. With the wearable network becoming more complex, fusion of the data from multiple, potentially heterogeneous, sensor sources becomes a nontrivial task that directly impacts performance of the activity monitoring applications. R. Gravina et. al. [10] discuss the state-of-the-art techniques on multisensor fusion in the BSN research area.

G. Fortino et. al. [11] analyze the requirements for an effective BSN specific software framework. They also present an open source programming framework, called SPINE (signal processing in node environment), designed to support

rapid and flexible prototyping and management of BSN applications.

S. Lokavée et. al. [12] proposed a sleep monitoring and gesture recognition system for patient based on polysomnography. This sensor pillow system employs a 3x3 sensor array of FSR (force sensing resistor) based on polymer thick film device for classifying and recognizing sleep posture. However, this work is only useful for point-of-care applications.

E. J. Pino et. al. [13] implemented a noninvasive sleep monitoring system using a bed pressure sensor array. The system detects changes in the contact pressure between a subject and the bed and is able to automatically select the sensor with the best respiratory signal, determine the respiratory rate, count number of sleep apneas, and count body position changes through the night. This work is similar to our approach except the smaller sensing area of 300 mm × 900 mm. However, they did not distinguish what posture a person is lying in.

L. Lin. et. al. [14] made a self-powered, highly sensitive, and fast responsive pressure sensor on the basis of the triboelectric effect. The pressure measurement range of the triboelectric active sensor (TEAS) was adjustable, which means both gentle pressure detection and large-scale pressure sensing were enabled. Through integrating multiple TEAS units into a sensor array, the as-fabricated TEAS matrix was capable of monitoring and mapping the local pressure distribution applied on the device with distinguishable spatial profiles. These nanogenerator-based active sensors are expected to replace FSR sensors in future applications.

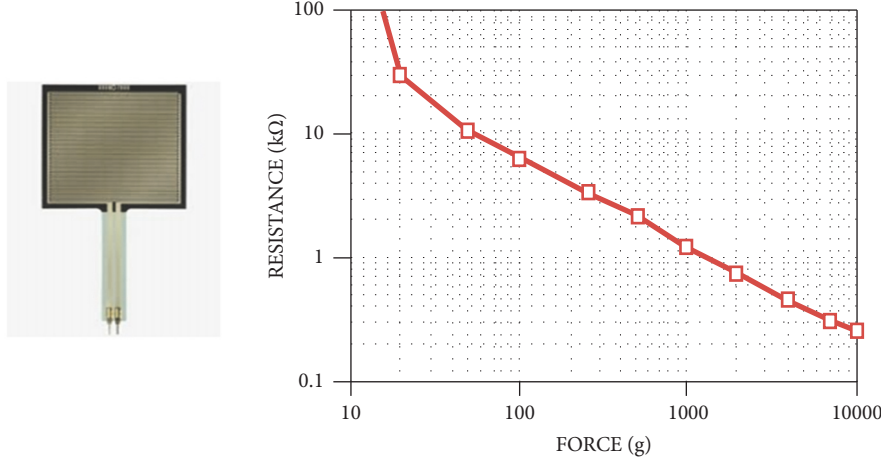


FIGURE 4: The FSR 406 sensor [18].

Lee [9] made a cotton mattress to implement the sleeping state sensing system which is installed with 64 pressure sensors and temperature sensors. He tried to detect unrighteous sleeping posture which disturbs a deep sleeping. He showed that there are little pressure changes over time for hip, waist, and head. On the contrary, legs and arms are not only relatively low in pressure, but also large in change. Unfortunately, he did not suggest a method to identify postures that interfere with comfortable sleep.

The following two papers are focused on detection of sitting posture. C. Ma et. al. [15] proposed a cushion-based posture recognition system to process pressure sensor signals for the detection of user's posture in the wheelchair. They compared five different machine learning approaches. They evaluated seven different classifiers to recognize five sitting postures. It is interesting for us that they deal with the optimal sensor placement problem. They investigated the contribution of each individual sensor to the recognition accuracy and determine the best sensor deployment using the backward selection method.

They [16] also proposed a method of activity classification and activity level assessment using a smart cushion to recognize sitting behavior. Two types of sensors are used to implement the cushion: six pressure sensors and a 9-axis inertial measurement unit. They calculated two features, standard deviation and approximate entropy, to recognize 5 sitting activities and 3 levels of sitting activities.

3. System Configuration

3.1. FSR Sensors. FSR sensors are devices that allow measuring static and dynamic forces applied to a contact surface [17]. Their specified switching time delay was 1 ms. The FSR 406 sensor in Figure 4 [18] is more sensitive to forces with lower magnitude, being able to distinctively respond to forces as low as 20 g [19]. Considering cheap and reliable force sensor, it can be a suitable candidate to measure the force during interaction [17].

In this paper, the FSR 406 sensor is used to measure pressure. As shown in Figure 4, it has a square shape and the

size of 45 mm × 45 mm. When the pressure is applied to it, it returns a resistance value that is inversely proportional to the pressure. The pressure range that can be measured by the FSR 406 sensor is from 0.1N to 10N. The pressure value sensed by the FSR sensor is stored as a digital value between 0 and 1,023.

3.2. The Smart Mat and the System Architecture. The prototype of a smart mat was manufactured to efficiently determine the lying posture. As shown in the left of Figure 5, a total of 128 FSR sensors are placed in the 16x8 grid structure. The spacing between the FSR sensors is 8 cm in both the horizontal and vertical direction in order to implement the prototype system with fewer pressure sensors. This has advantages in terms of economic cost and power consumption. The narrower the spacing between the sensors is, the more accurate the pressure measurement will be possible. In order to confirm this, a comparative experiment was conducted by making an additional smart mat with 6 cm spacing. The experimental results show that the number of FSR sensors which measured the pressure is increased by 13% as compared with the case where they were arranged at the spacing of 8 cm. A relationship between the sensor spacing and the performance of lying posture determination will be conducted in a future study.

The smart mat is placed between the sheet and the mattress. It is designed to fit the size of a hospital bed and thus its size is 189.9cm x 90.9cm. It is divided into four sections, each consisting of a total of 32 (4 rows x 8 columns) FSR sensors. These four sections are managed by the corresponding four independent controllers implemented with Arduino Mega boards. These controllers are hardwired to the concentrator implemented with Raspberry pi 3 board [20, 21]. It serves as a buffer to temporarily store the collected sensing data and wirelessly transmits them to the long-term care monitoring system (LCMS) at regular intervals. The LCMS uses MySQL as DBMS [22]. In the prototype system, wireless LAN (IEEE 802.11b) is used for ease of implementation, but the wireless transmission protocol could be changed according to application purpose. Figure 6 shows the process flow of the proposed smart care system.

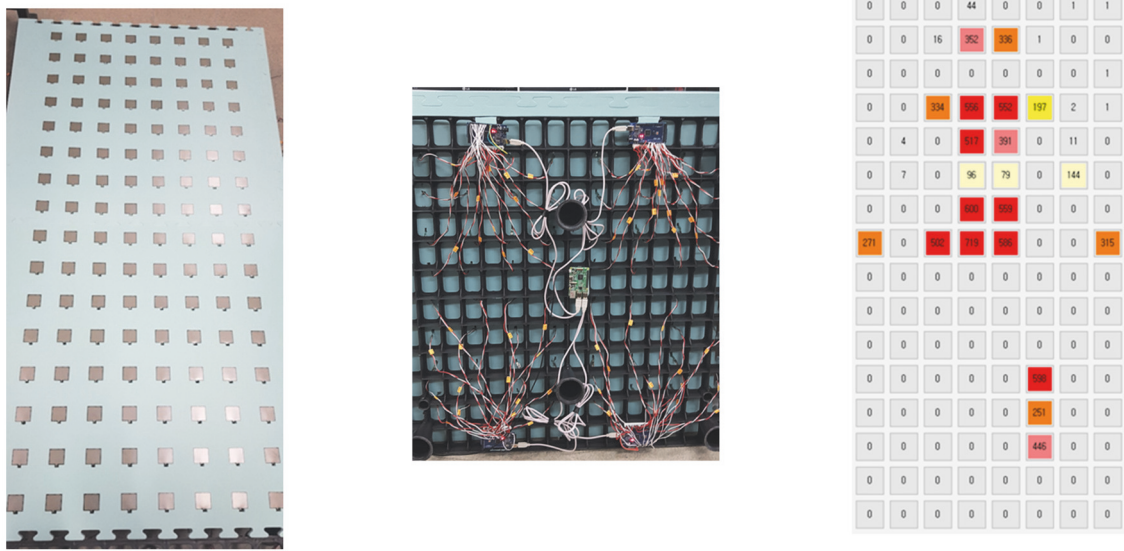


FIGURE 5: The 16x8 smart mat prototype (*left*); the hardware of a single section behind the mat (*center*); and the snapshot of the sensed pressures at each sensor (*right*).

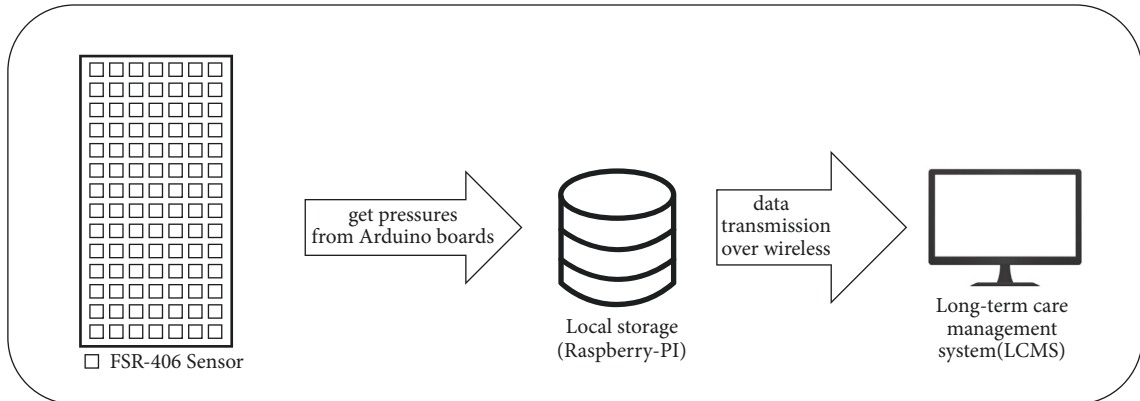


FIGURE 6: The process flow of the proposed smart care system.

3.3. The Classification of Body Parts. In order to determine the lying posture with a limited number of FSR sensors, it is necessary to decide which body part should be identified first. Some body parts move frequently, so the pressure is not measured properly. For instance, *hands* and *feet* have low pressure intensity and short pressure duration. The shorter the pressure duration, the greater the variation in the pressure value, making it difficult to identify the body part. However, *head*, *shoulders*, and *hips* are the protruding parts, and the pressure in these parts is measured stronger than other parts. In addition, they have a long duration of pressure because of their less movement.

Based on the pressure value and the duration, the body parts can be divided into three tiers as shown in Table 1. The body parts belonging to the tier-1 are relatively easy to recognize and would suggest a way to determine the lying posture based on them.

Table 1 lists the body parts according to the classification criteria, the *threshold* and the *duration*. Notice that these

values are obtained from the experiments. In the experiments, the sampling period was set to be fixed as 1 minute. In actual situations, the pressure may vary depending on how close the body part is to the FSR sensors.

Standard body dimensions help determine body parts more effectively. The definitions of the body dimensions referenced in this paper are shown in Figure 7.

3.4. Data Mapping and Sampling Period. The data sent to the LCMS system is mapped one to one in a two-dimensional array, identical to the grid structure of the smart mat. That is, the position (*i*-th row, *j*-th column) of the FSR sensor corresponds to the index (*i*, *j*) of the array. The interval for measuring the pressure of the smart mat, called sampling period, is initially set to one minute. However, the sampling period may be adjusted variably depending on the rate of change in the pressure value. If the number of the FSR sensors whose values are changed is less than 10% (i.e., the number of the sensors is 12), it is increased by 30 seconds. The maximum

TABLE 1: The threshold and the duration for each tier.

tier	threshold	duration	body parts
1	500>	>5 minutes	head, shoulders, hip
2	200~600	1~5 minutes	thigh, calf
3	100~499	< 1 minutes	hands, arms, legs, feet

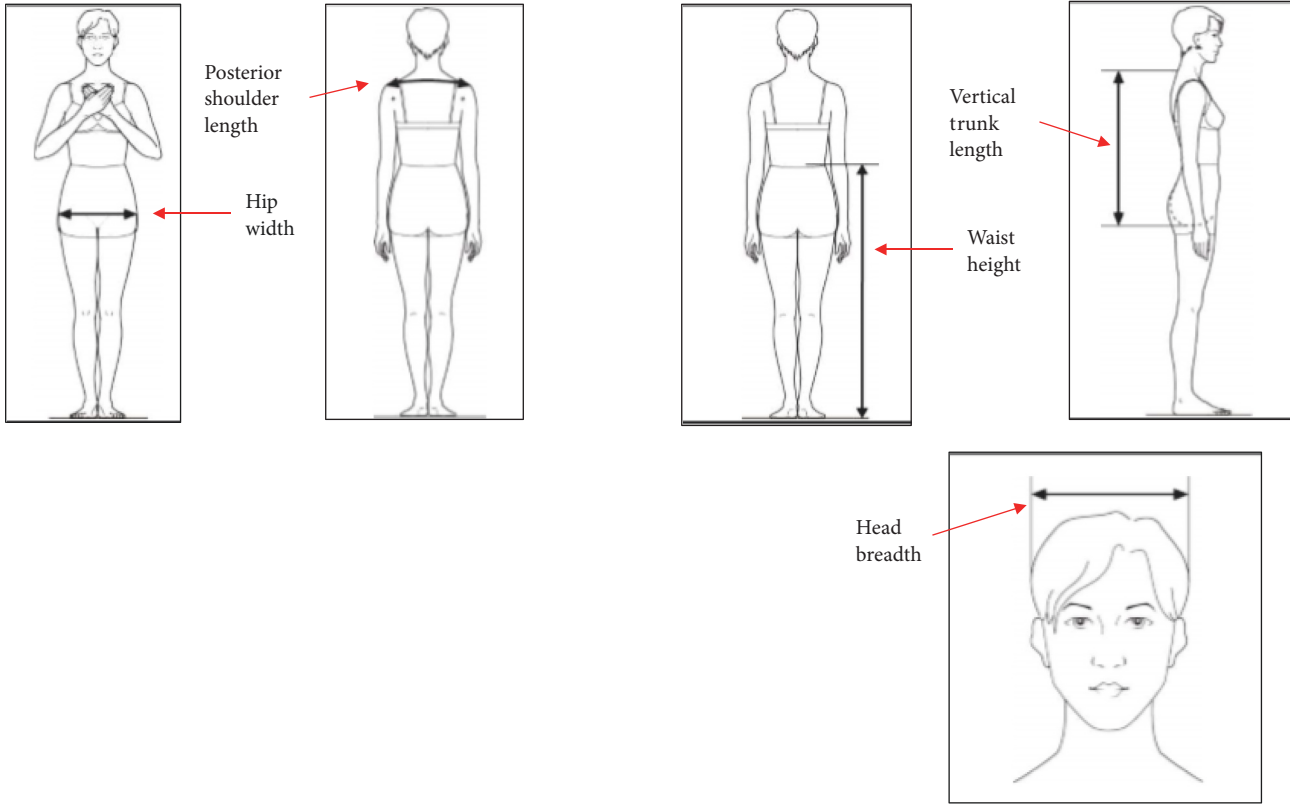


FIGURE 7: The definitions of the selected body dimensions [23].

sampling period is 5 minutes. The sampling period can be adjusted according to individual sleep patterns.

4. The Algorithm for Discriminating Lying Posture in a Bed

The posture discrimination algorithm to be proposed in this paper determines the lying posture based on the body parts corresponding to the tier-1. To find them, it will apply a different size filter for each body part. The filter size is determined considering the pressure distribution of the body part to be identified. A filter is used to calculate the cumulative sum of the pressure of the FSR sensors in the area that it occupies. The search space can be properly restricted taking into account the physical characteristics of the body part. The cumulative sums are obtained by sequentially moving the filter within a specified search space. The filter area having the largest value is determined as a corresponding body part. Depending on the position of the tier-1 body parts found and the overlapping patterns among them, it determines the lying posture of a person in the bed.

4.1. Determination of Filter Size according to the Characteristics of the Tier-1 Body Part. A square-shaped FSR-406 sensor with a side length of r is called a *cell*. Let w and h be the horizontal and vertical spacing between cells, respectively, as shown in the left of Figure 8. The filter size is determined by the number of cells contained in the row and column of the filter. When the 3x2 filter is applied as shown in the right of Figure 8, the measurable physical space becomes $3(r+w) \times 2(r+h)$. For $w = h = 8\text{ cm}$, $r = 4.5\text{ cm}$, the measurable area when applying the 3x2 filter is $37.5\text{cm} \times 25.0\text{cm}$.

The filters to recognize the body parts belonging to the tier-1 are shown in Table 2. The filter size was determined by analyzing the Korean body dimensions [23] and the pressure distribution obtained from the experiments. For example, in the case of a *hip*, the width that can be measured by the filter is slightly smaller than the actual body dimension, but the pressure at both ends of the hip is measured lower. Weights can be assigned to account for individual body characteristics. In this paper, all the weights are set equal to 1.

4.2. The Lying Posture Discrimination Algorithm. The flowchart for the lying posture discrimination algorithm is shown

TABLE 2: The body parts and the corresponding filter size (unit: mm).

the tier-1 body part	filter size	Measurable length	body dimension (average)
shoulder	3x2	375(width)	<i>posterior shoulder length</i> 370(women)~421(men)
hip	2x2	250(width)	<i>hip width</i> 326(women)~329(men)
head	1x1	125(width)	<i>head breadth</i> 151(women)~159(men)

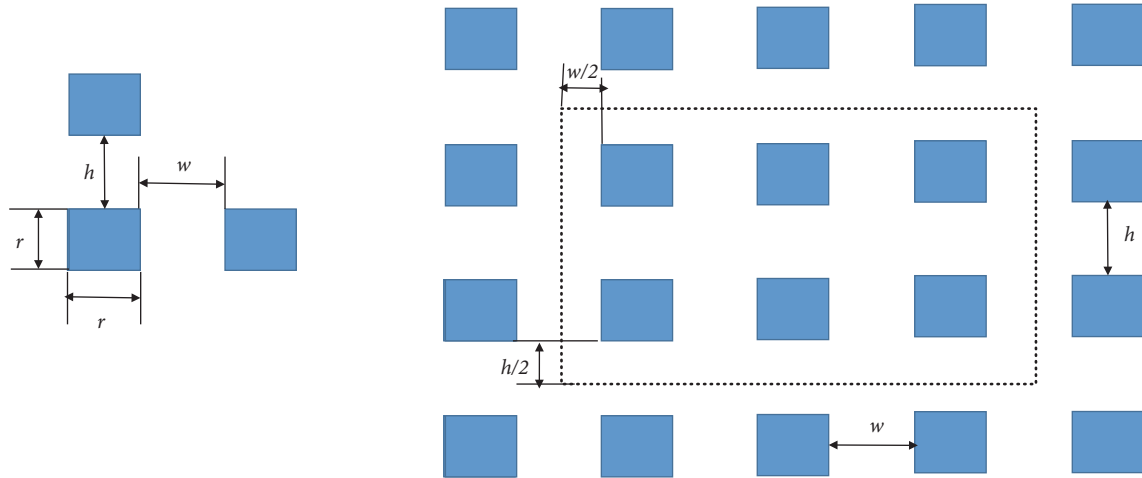


FIGURE 8: The horizontal and the vertical distance between FSR sensors (left) and the measurable area by using the 3x2 filter (right).

as Figure 9. Notice that the state of sitting on the bed or sitting on one side of the bed is not included in the posture discrimination because it can be easily distinguished only by the pressure distribution. Based on the pressure distribution for a certain period of time, it is confirmed whether the person is lying on the bed, and from this time the lying posture discrimination algorithm is applied.

First of all, the proposed algorithm finds the body parts that belong to the tier-1. The sequence of the body parts to be found is shoulder → hips → head.

Step 1. Find the shoulder using the 3x2 filter.

Step 2. Find the hips using the 2x2 filter.

Step 3. Find the head using the 1x1 filter.

The reason to look for the shoulder first is because it has the widest area and has the longest pressure duration, so it is relatively easy to distinguish among them. It is advantageous to distinguish the hip because it has a wide area of pressure and long duration of pressure. That is, the possibility of misjudging the body part is relatively low. After finding the shoulder and the hips, it can find the head by limiting the search space in the opposite direction of hip.

In the next step, it determines whether a person is lying in either prone or nonprone posture. In the prone posture, the cumulative sum ref_{hip} of pressures in the hip area is smaller than one in the nonprone postures. After that, it determines the lying posture by considering whether the three body parts

overlap. It is intuitive to judge what the posture is when the extended shoulder area does not overlap with either the hip or the head as shown in Figure 2. However, if the extended area overlaps with both as shown in Figure 3, it should be required to determine the lying postures based on the pressure distribution.

The cumulative sum of the left four columns L_c and the cumulative sum of the right four columns R_c are used as information for determining the posture. $L_c \gg R_c$ means that the upper body is pointing to the left, while $L_c \ll R_c$ means that it is pointing to the right. On the other hand, if a person is lying in the upright posture, the difference between L_c and R_c is within the threshold. Notice that the threshold value will be determined empirically.

4.2.1. Shoulder Discrimination. The proposed algorithm applies the 3x2 filter according to Table 2 for shoulder discrimination. $p_{i,j}$ in Figure 10 is the pressure value sensed in the cell (i, j) and has a value between 0 and 1,023. The filter in Figure 10 can be expressed as $[R_i, C_j : R_{i+1}, C_{j+2}]$, where R and C indicate the row and the column of the smart mat, respectively. In the filter, the reference cell is the cell (i, j) .

For all the cells in the filter, it calculates the cumulative sum of the pressure $p_{i,j}$ multiplied by the weight $w_{i,j}$. Notice that all the weights are set equal to 1. The cumulative sum $z_{i,j}$ of the filter is obtained on the basis of the reference cell.

$$z_{i,j} = \sum_{m=n=0}^{m=2,n=1} (p_{i+m,j+n} \times w_{m,n}) \quad (1)$$

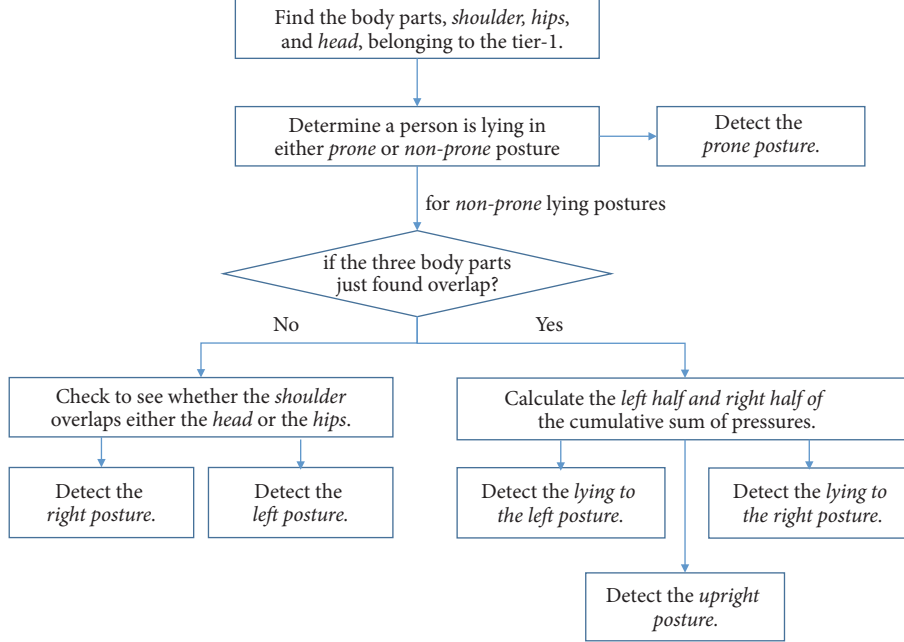


FIGURE 9: The flowchart of the lying posture discrimination algorithm.



FIGURE 10: The 3x2 filter.

TABLE 3: The body dimensions and the average values used to find the shoulder.

body dimension	average (ages from 16 to 69)	
sitting height	men	927
	women	866
elbow height - sitting	men	264
	women	253

If the number of rows and the number of columns to search are N_R and N_C , respectively, and the filter size is $L \times W$, then the value of cumulative sum obtained by applying the filter is $(N_R - L + 1)(N_C - W + 1)$. Then the filter $z_{selected}$ having the maximum value can be obtained.

$$z_{selected} = \max_{i \in (1, N_R - R + 1), j \in (1, N_C - W + 1)} z_{i,j} \quad (2)$$

To determine the search space to apply the 3x2 filter, we use the *sitting height* and the *elbow height sitting* of the body dimension as shown in Table 3. That is, there is a shoulder part in the region where the *sitting height* is subtracted from the *elbow height sitting*, which is smaller than 613 mm (women, in average) to 663 mm (men, in average). Therefore, it is sufficient to search only six rows (125mm x 6 cells = 750 mm) of the smart mat. When lying is in the upright posture, the

pressure in each cell is sensed as shown in Figure 11. There are two search areas for finding the shoulder part: [R1: C1, R5: C8] and [R12: C1, R16: C8]. Since we do not know in which direction a person is lying, we should include both of these in the search space.

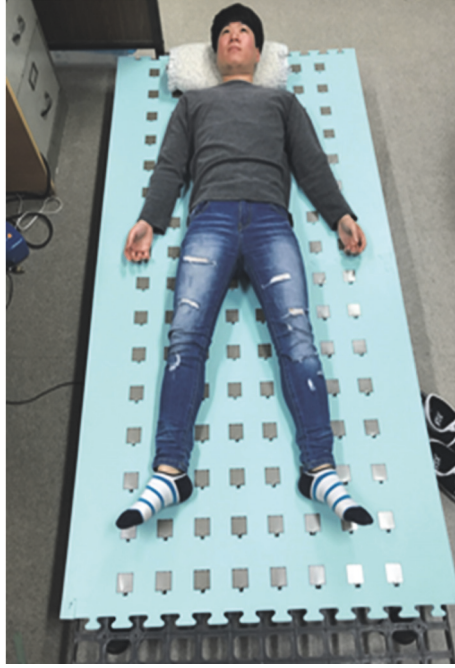
Table 4 shows the result of applying 3x2 filter to the above search spaces. The area with the maximum value as a result of applying the 3x2 filter is [R4:C3, R5: C5]. The area $[R_{sh} : C_{sh}, R_{sh+1} : C_{sh+2}]$ is identified as the *shoulder*.

$$z_{selected} = z_{4,3} = \sum_{m=n=0}^{m=2, n=1} (p_{4+m, 4+n} \times w_{m,n}) \quad (3)$$

4.2.2. Hip Discrimination. The search space for hips can be effectively limited based on the vertical trunk length (men 690.6 mm, women 621 mm). Because the shoulder already occupies two cells (25mm), the actual search space can be restricted to up to five cells (625mm). As with the shoulder discrimination, the upper and lower two regions must be searched independently. The minimum distance criteria can be applied since the hips are searched with the shoulders discriminated. That is, the minimum length is the distance obtained by subtracting the hip vertical length (called *body rise*, 231 mm (women) to 261 mm (men)) from the *vertical trunk length*. In other words, the minimum distance is 390

TABLE 4: The results of applying the 3x2 filter to the upper (a) and the lower (b) search space to discriminate the shoulder.

	(a)					
	1	2	3	4	5	6
1	16	412	748	733	338	3
2	16	368	704	689	337	2
3	334	890	1442	1305	751	201
4	338	1411	2350	2213	1153	211
5	11	624	1083	1083	625	155
	(b)					
	1	2	3	4	5	6
11	0	0	0	598	598	598
12	0	0	0	849	849	849
13	0	0	0	697	697	697
14	0	0	0	446	446	446
15	0	0	0	0	0	0



	C1	C2	C3	C4	C5	C6	C7	C8
R1	0	0	0	44	0	0	1	1
R2	0	0	16	352	336	1	0	0
R3	0	0	0	0	0	0	0	1
R4	0	0	334	556	552	197	2	1
R5	0	4	0	517	391	0	11	0
R6	0	7	0	96	79	0	144	0
R7	0	0	0	600	559	0	0	0
R8	271	0	502	719	586	0	0	315
R9	0	0	0	0	0	0	0	0
R10	0	0	0	0	0	0	0	0
R11	0	0	0	0	0	0	0	0
R12	0	0	0	0	0	598	0	0
R13	0	0	0	0	0	251	0	0
R14	0	0	0	0	0	446	0	0
R15	0	0	0	0	0	0	0	0
R16	0	0	0	0	0	0	0	0

FIGURE 11: The upright posture (left) and the values sensed by the 16x8 FSR sensors (right).

mm to 429 mm and should be more than 3 cells (375mm). Therefore, there are two search areas for finding the shoulder part: $[R_{sh+3} : C1, R_{sh+5} : C8]$ and $[R_{sh-2} : C1, R_{sh-5} : C8]$.

Table 5 shows the result of applying 2x2 filter to the above search spaces. As a result of applying the 2x2 filter, the area having the maximum value is [R7:C4, R8:C5]. The area $[R_{hip} : C_{hip}, R_{hip+1} : C_{hip+1}]$ is identified as the *hips*.

4.2.3. Head Discrimination. The head is at least the length of the neck away from the shoulder. Therefore, the row that is at least 1-cell away from the shoulder found above can be searched by 1x1 filter. In addition, since the shoulder and the hips are discriminated, the search space for finding the head can be restricted to one direction. The algorithm searches

for the space in the opposite direction to the hips to find the head. If $R_{sh} - R_{hip} > 0$, then the search space becomes $[R_{sh+3} : C1, R_{sh+3} : C8]$, and if $R_{sh} - R_{hip} < 0$, the search space becomes $[R_{sh-2} : C1, R_{sh-2} : C8]$.

In the case of Figure 8, the search region for head discrimination is [R2: C1, R2: C8]. Table 6 shows the result of applying 1x1 filter to the above search spaces. As a result of applying the 1x1 filter, the area having the maximum value is [R2:C4]. The area $[R_{head} : C_{head}]$ is identified as the *head*.

4.2.4. Determination of Lying Posture. Figure 12 shows the pressure distribution when lying down in four different postures. The body part discrimination algorithm described above is applied to find shoulder, hips, and head, and the

TABLE 5: The results of applying the 2x2 filter to the upper (a) and the lower (b) search spaces to discriminate the hips.

(a)							
	1	2	3	4	5	6	7
1	0	16	412	732	337	2	2
2	0	16	368	688	337	1	1
(b)							
	1	2	3	4	5	6	7
7	271	502	1821	2464	1145	0	315
8	271	502	1221	1305	586	0	315
9	0	0	0	0	0	0	0

TABLE 6: The results of applying the 1x1 filter to the single row to discriminate the head.

	1	2	3	4	5	6	7	8
1	0	0	16	352	336	1	0	0

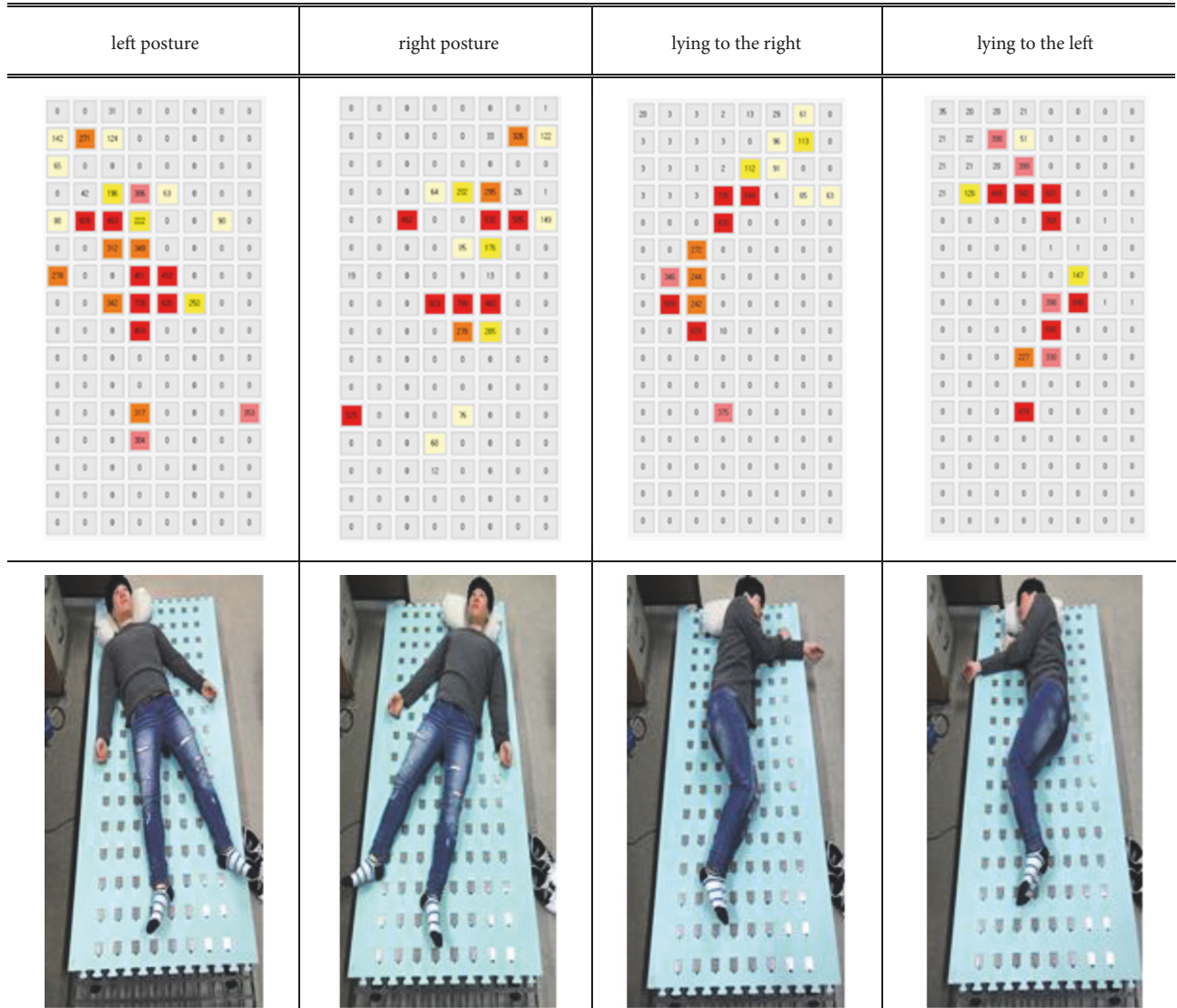


FIGURE 12: The different lying postures and the corresponding pressure distributions.

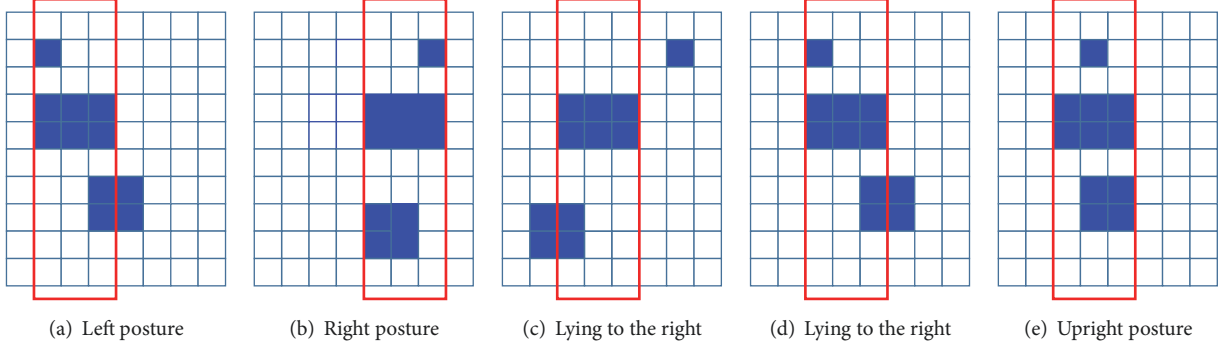


FIGURE 13: The lying posture discrimination by the coverage of the shoulder area.

TABLE 7: The L_c , R_c , and the difference with respect to lying posture.

	upright posture	left posture	right posture	lying to the right	lying to the left
L_c	4018	6251	1753	3922	2888
R_c	4472	1843	4373	1193	3692
$L_c - R_c$	+454	+4408	-2620	+2729	-804

results of the discrimination of the corresponding body parts are shown in Figure 13.

The basic idea of the posture determination algorithm is to identify the upright posture if the head, the shoulder, and the hips are on a straight line. That is, if the shoulder area (3×2) completely includes the hip area (2×2) and the head area (1×1) as shown in Figure 13(e), the algorithm determines that a person lies in an upright posture. If the shoulder area does not fully cover the hips and the head region, it is judged in the supine posture. If the right part of the hip area overlaps the shoulder area, it is judged to be either the right posture (Figure 13(b)) or lying to the right (Figure 13(c)). If the left part of the hip area overlaps with the shoulder area, it is judged to be either the left posture (Figure 13(a)) or lying to the left (Figure 13(d)).

However, as shown in the Figure 13(b), even when lying straight up but twisted leftward or rightward, the shoulder area completely covers the head and the hip area. It is difficult to determine the exact posture simply by identifying the lying posture only by the shoulder region including the two body regions.

To do this, it calculates the cumulative sum $S_{C_i} = \sum_{i=1}^{16} (p_{i,j} \times w_{i,j})$ of pressures at each column. The cumulative sum $L_c = \sum_{j=1}^4 \sum_{i=1}^{16} (p_{i,j} \times w_{i,j})$ of the left four columns and the cumulative sum $R_c = \sum_{j=5}^8 \sum_{i=1}^{16} (p_{i,j} \times w_{i,j})$ of the right four columns are used as information for determining the posture. The method of determining the lying posture using these two values has already been described above. Notice that the typical value of the threshold is 500. As summarized in Table 7 it can be seen that the difference between L_c and R_c is closely related to the lying posture.

Figure 14 shows the snapshot of the distribution of the cumulative pressure sum of each column of the smart mat for each lying posture. The pressure distribution is clearly different for each lying position.

4.2.5. Discrimination between Upright Posture and Prone Posture. Figure 15 shows the pressure distribution when lying down in a prone posture. The most distinctive difference between the upright posture and the prone posture is that the cumulative sum of the pressure of the hip is below the reference value ref_{hip} (the typical value is 1,000). Notice that the area of the hip to be found is defined as $[R_{hip} : C_{hip}, R_{hip+1} : C_{hip+1}]$. In other lying postures, the cumulative sum of pressure on the hips is greater than 1,000, but less than 1,000 in the prone position. Therefore, after examining the inclusion of the shoulder area, it is checked whether or not the cumulative sum of the pressure on the hip area is below 1,000 or higher to determine whether it is an upright or a prone position.

4.2.6. Discrimination of Other Body Parts. When *heel* is in a fixed posture and it is located at the position of the FSR sensors, the pressure is sensed relatively high. Knowing the area of the head and the heel allows us to estimate the height of the person lying down. However, it is not easy to distinguish the heel at once because it moves frequently. Therefore, it is necessary to get at least three consecutive pressure distributions to discriminate the heel. This results in a delay in the recognition of heel compared to other body parts. The 1×1 filter can be used for heel recognition.

The pressure on *hands* can also be measured in a similar way to the heel. *Feet* and *arms* are similar to heel and hand. Because they also frequently move, it is possible to identify them by analyzing at least three pressure distributions continuously. Most of the body parts that do not belong to the tier-1 have a high frequency of movement, and depending on where they are located, the FSR sensors may not be able to detect any pressure. Therefore, measurements should be made several times over a certain period of time. In this paper, we will not discuss in detail the other parts determination because it does not seriously affect the posture determination.

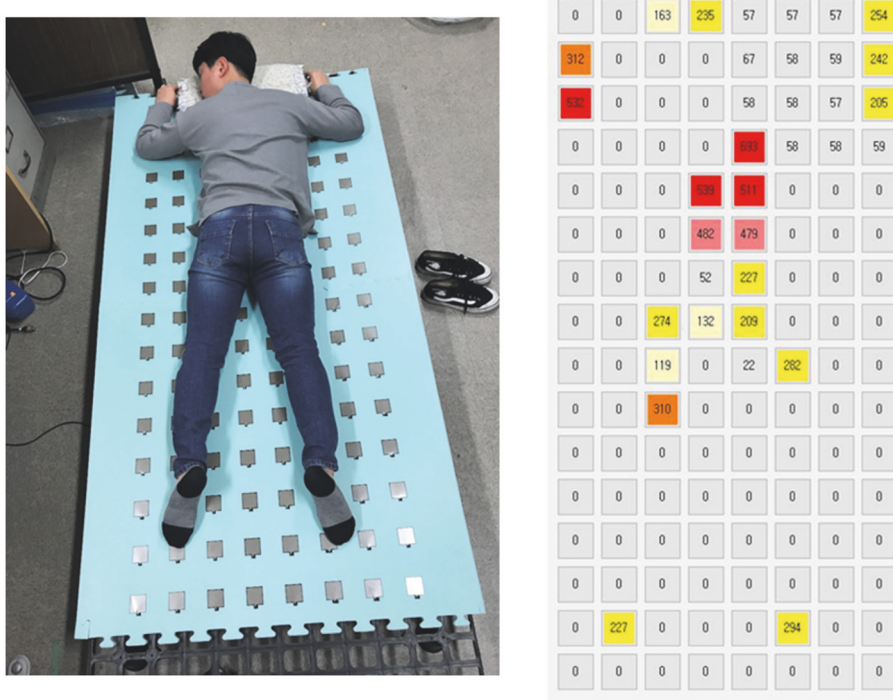


FIGURE 14: The prone posture (*left*) and the values sensed by 16x8 FSR sensors (*right*).

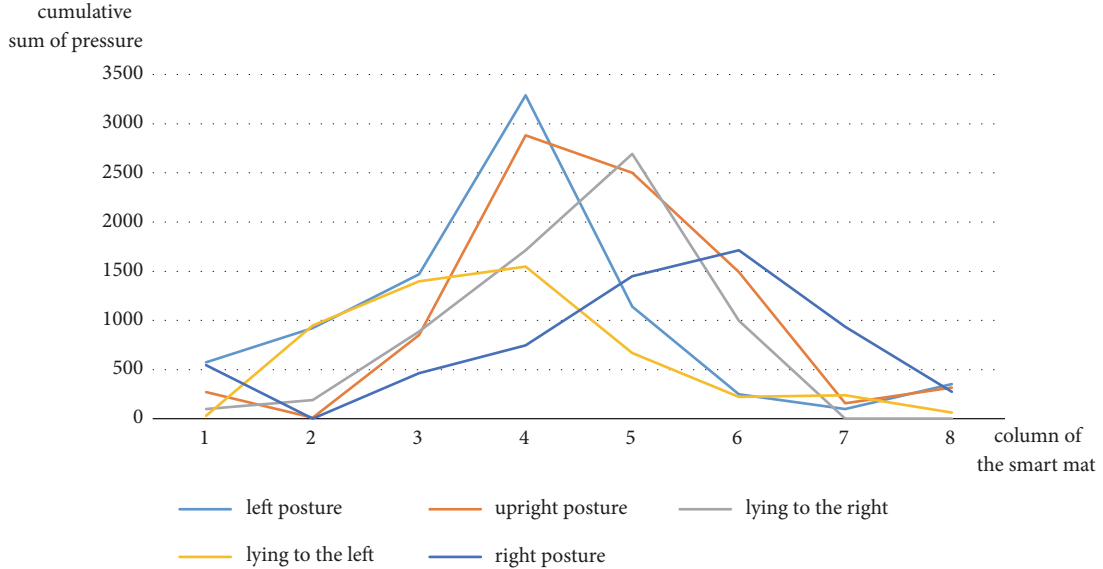


FIGURE 15: The cumulative sum of pressure in each column with respect to the lying postures.

5. Experimental Results

5.1. Experiment Setup. Although the spacing between the FSR sensors has a significant effect on the posture determination, the horizontal and vertical spacing between the sensors is 8 cm apart for ease of implementation. The sampling interval for obtaining the pressure distribution from the smart mat is at least 1 minute and up to 5 minutes. It is variably adjusted according to the frequency of the movement of the

person lying down. To increase the accuracy of the posture determination, the average of the pressure distributions sampled at least three times is used. Therefore, the time taken to discriminate the posture is determined by the sampling interval and the number of times the pressure distribution is used. In most experiments, the posture was determined using a total of three pressure distributions at the sampling interval of 1 minute. In this case, the lying posture was judged in about 3 minutes.

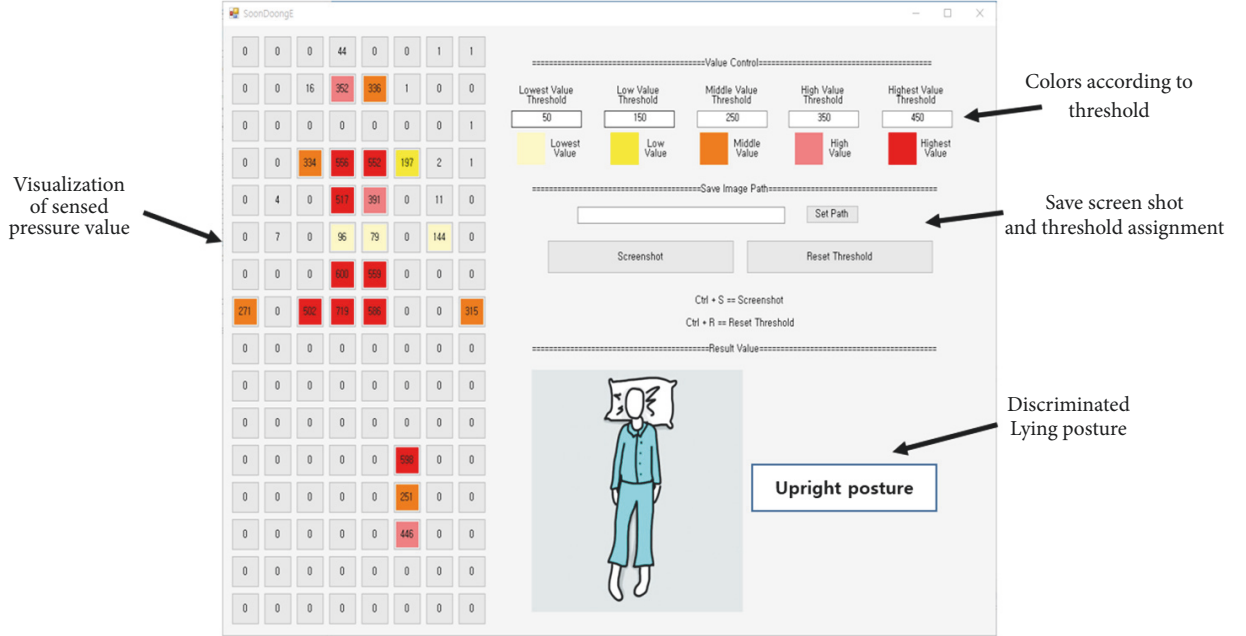


FIGURE 16: The screen configuration of the lying posture discrimination system.

As shown in Figure 16, the five colors are displayed for visualization of the pressure, and the threshold can be specified for color coding. In the experiment, the colors were classified into 5 areas such as 50~149, 150~249, 250~349, 350~449, 450, or more depending on the pressure values. The screen configuration of the implemented system is shown in Figure 16.

The proposed algorithm identifies six postures: *upright* posture, *left* posture, *right* posture, *lying to the left*, *lying to the right*, and *prone* posture. The posture discrimination begins after 5 minutes (*adjustable*) from the time where the pressure distribution is concentrated and then dispersed. The algorithm stops the posture discrimination when the pressure distribution is concentrated in one place.

5.2. Recognition Rate with respect to the Number of Samplings. Six men (age 23-67, height 162 ~ 175 cm, weight 58 ~ 75 kg) and one woman (age 63 years, height 155Cm, weight 47 Kg) were measured for 3 hours. The subjects' postures were verified by capturing the lying images at the time of the discrimination. The average number of postures taken by the subject during each measurement was 40, and there were about 13 postures per hour.

The pressure distribution obtained through a single sampling shows that the pressure in body parts is not properly measured. However, increasing the number of times of sampling can measure the pressure in body parts that have not been sensed. That is, increasing the number of samples and obtaining the average value for each cell gives a constant shape to the pressure distribution curve.

Figure 17 shows how the pressure distribution varies with the number of samples in the right posture and in the upright posture. We set the sampling interval to 60 seconds to

effectively control the amount of data collected and managed, since there is little movement of the body during bedtime. Thus, in Figure 17, 0, 60 seconds, 120 seconds, 180 seconds, and 240 seconds refer to single sampling, double sampling, three-time sampling, four-time sampling, and five-time sampling, respectively. The curve for each sampling represents the average value for the sampling. Notice that C_1, C_2, \dots, C_8 in Figure 14 refer to each row of the smart mat. As shown in Figure 14, the approach to higher-order sampling shows that the variation in the graph decreases.

As summarized in Table 8, a total of 258 posture determinations were attempted. The recognition rate was about 90% when five samplings were used. N_1 , N_3 , and N_5 are the number of times of successful posture determination with one sampling, three samplings, and five samplings, respectively.

Recognition failure occurred mainly in left posture, lying to the left posture, right posture, and lying to the right posture. This is due to the fact that the change in pressure distribution due to movement in the process of changing posture has increased. The accuracy in posture discrimination becomes very high when one posture is kept long. The recognition rate will be improved if the spacing between the FSR sensors is narrowed.

Figures 18 and 19 show the changes in the cumulative pressure values for each column when lying in the upright posture and the right posture for 5 minutes. As can be seen in Figure 18, the person was lying in columns C_1 , C_2 , and C_3 with an upright posture. As time elapses, the posture was moved toward column C_4 . It can be seen that the cumulative value of the column C_3 maintains a remarkably large value. However, when lying in the right posture, the values of all the columns except C_7 and C_8 are significantly changing as shown in Figure 19. The characteristics of pressure change

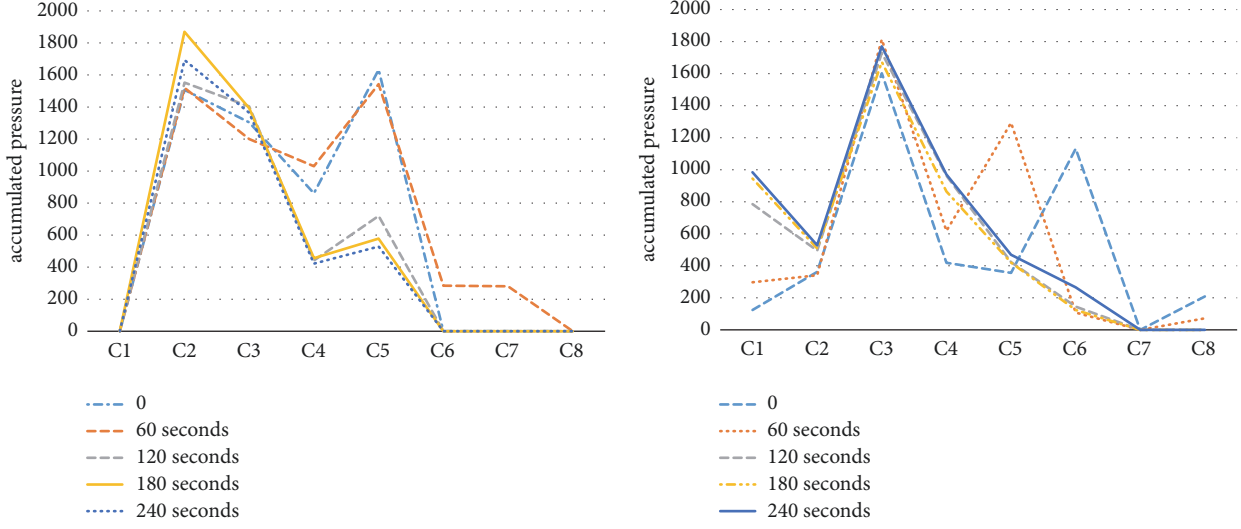


FIGURE 17: The pressure distribution curve for the number of samplings: right posture (left) and upright posture (right).

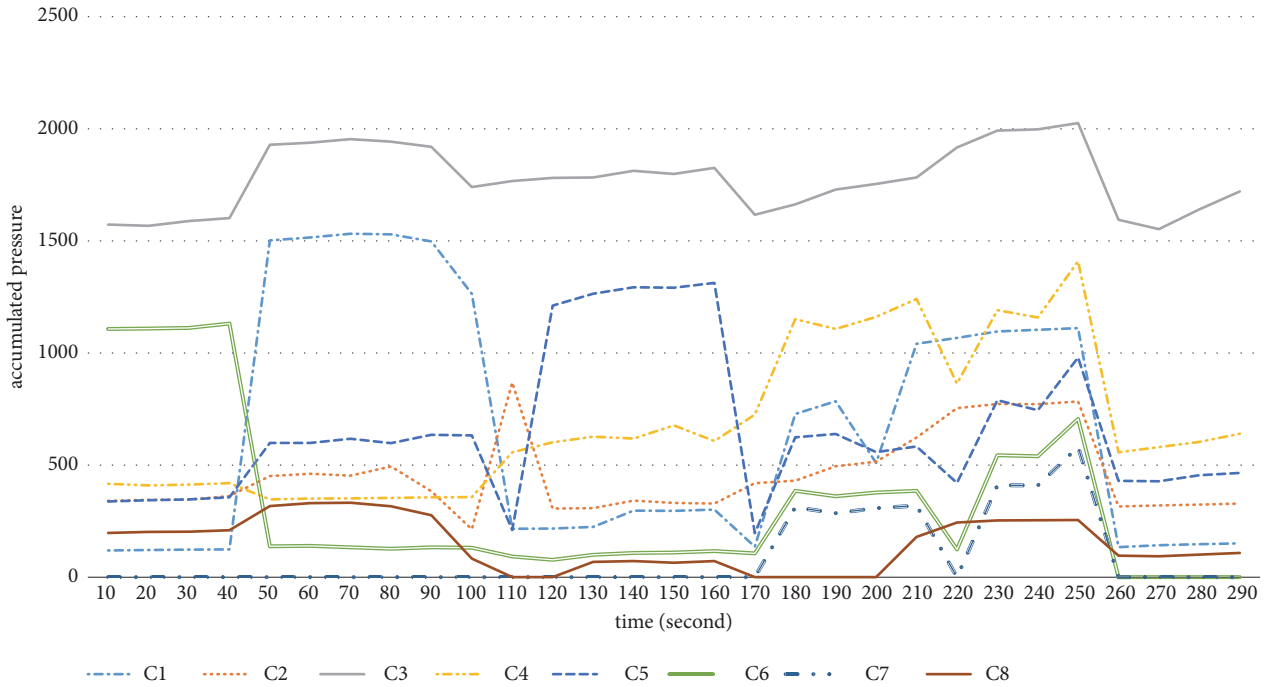


FIGURE 18: The pressure distribution curve for each column in the upright posture.

TABLE 8: Determination of the lying posture with respect to the number of samplings.

posture	Total no of postures	with 1 sample		recognition rate			
		N_1	Ratio(%)	N_3	Ratio(%)	N_5	Ratio(%)
upright	72	64	88.9	67	93.1	68	95.8
prone posture	49	35	71.4	41	83.7	42	85.7
prone posture	51	35	68.6	43	84.3	45	88.2
lie to the left	33	24	72.7	27	81.8	29	87.9
lie to the right	39	27	69.2	33	84.6	33	84.6
prone posture	14	13	92.9	14	100.0	14	100.0
sum	258	198	77.2(avg.)	225	87.9(avg.)	231	90.4(avg.)

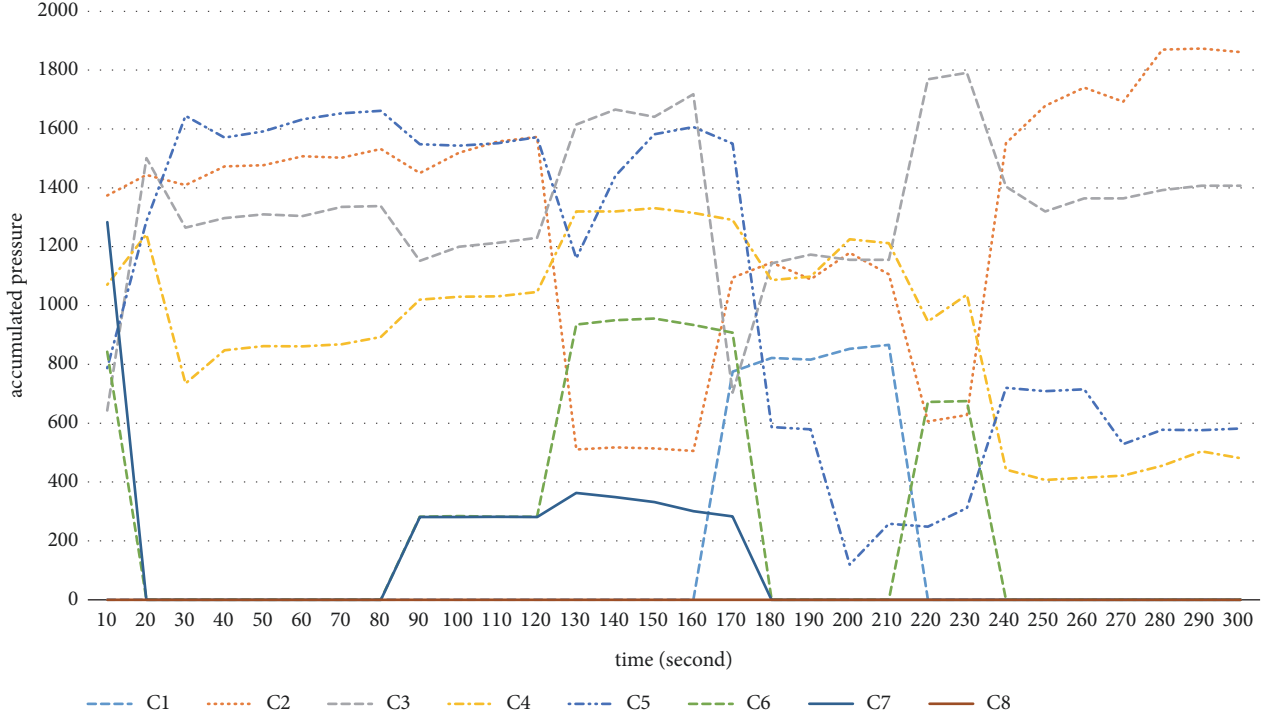


FIGURE 19: The pressure distribution curve for each column in the right posture.

by posture are expected to be useful when machine learning method is introduced in the near future.

6. Conclusions

We have implemented a smart bed system to determine human's lying postures using FSR sensors arranged in a grid structure. We define *head*, *shoulder*, and *hips* as tier-1, which have low movement and large pressure range in human body parts. We investigated the correlation of these body parts belonging to the tier-1 and proposed an algorithm to determine the lying position. Also, the pressure distribution in the *left-half* and *right-half* regions of the smart bed is reflected in the posture discrimination process so as to increase the accuracy of the discrimination. Since the pressure is measured only when the body part is placed in the position where the FSR sensor is located, the accuracy of discrimination can be improved by increasing the number of samples of the pressure distribution.

Experimental results show that the accuracy of posture discrimination reached 90%, when the posture was determined at intervals of five minutes by increasing the number of samples up to five. Most of the posture discrimination errors occurred in the process of changing the lying posture, for example, *lying to the left* posture to the *left posture*.

When the spacing between the FSR sensors is narrowed, it is expected that the accuracy of the discrimination will be improved because a more detailed pressure distribution can be obtained. In addition, the analysis of the pressure distribution by each column of the smart mat showed that distinct features were extracted for each posture. It is expected that the measured data set from this research can be used as a

training set to achieve improved results by applying machine learning techniques. This system can be used for sleep posture monitoring or behavior pattern monitoring.

Data Availability

The JSON or CSV data, except the personal information, used to support the findings of this study are available from the corresponding author upon request.

Conflicts of Interest

The authors declare that there are no conflicts of interest regarding the publication of this paper.

Acknowledgments

This work is supported by the 2013 Grant of Incheon National University.

References

- [1] Population and housing census, Statistics Korea, <http://www.census.go.kr/>.
- [2] H. Yeon-ok, "Geriatric care facilities: Recent trends in risk management," *Journal of the Korean Gerontological Society*, vol. 26, no. 3, pp. 505–520, 2006.
- [3] Y. S. Delahoz and M. A. Labrador, "Survey on fall detection and fall prevention using wearable and external sensors," *Sensors*, vol. 14, no. 10, pp. 19806–19842, 2014.
- [4] G. D. Velhal, "Domestic accidents among the elderly," *Annals of Tropical Medicine and Public Health*, vol. 5, no. 2, pp. 61–62, 2012.

- [5] M. Sartini, M. L. Cristina, A. M. Spagnolo et al., "The epidemiology of domestic injurious falls in a community dwelling elderly population: An outgrowing economic burden," *European Journal of Public Health*, vol. 20, no. 5, pp. 604–606, 2010.
- [6] Symptoms of Pressure Ulcers, <http://www.nhs.uk/Conditions/Pressure-ulcers/Pages/Symptoms.aspx>.
- [7] T. Yoshikawa, N. J. Livesley, and A. W. Chow, "Infected pressure ulcers in elderly individuals," *Clinical Infectious Diseases*, vol. 35, no. 11, pp. 1390–1396, 2002.
- [8] Research Topic: Anthropometry - Identification of Body Measures (Human Body Kinematic & Dynamic Parameters), Robotics Laboratory, <http://www.pupin.rs/RnDProfile/research-top-ic12.html>.
- [9] S. Lee, *A Study of Sleeping State Sensing System, [Master, thesis]*, Dankook University, 2009.
- [10] R. Gravina, P. Alinia, H. Ghasemzadeh, and G. Fortino, "Multi-sensor fusion in body sensor networks: State-of-the-art and research challenges," *Information Fusion*, vol. 35, pp. 68–80, 2017.
- [11] G. Fortino, R. Giannantonio, R. Gravina, P. Kuryloski, and R. Jafari, "Enabling effective programming and flexible management of efficient body sensor network applications," *IEEE Transactions on Human-Machine Systems*, vol. 43, no. 1, pp. 115–133, 2013.
- [12] S. Lokavee, N. Watthanawisuth, J. P. Mensing, and T. Kerdcharoen, "Sensor pillow system: Monitoring cardio-respiratory and posture movements during sleep," in *Proceedings of the 4th Biomedical Engineering International Conference, BMEICON-2011*, pp. 71–75, Thailand, January 2012.
- [13] E. J. Pino, A. Dorner de la Paz, P. Aqueveque, J. A. Chavez, and A. A. Moran, "Contact pressure monitoring device for sleep studies," in *Proceedings of the 35th Annual International Conference of the IEEE Engineering in Medicine and Biology Society (EMBC)*, pp. 4160–4163, Osaka, Japan, July 2013.
- [14] L. Lin, Y. N. Xie, S. H. Wang et al., "Triboelectric active sensor array for self-powered static and dynamic pressure detection and tactile imaging," *ACS Nano*, vol. 7, no. 9, pp. 8266–8274, 2013.
- [15] C. Ma, W. Li, R. Gravina, and G. Fortino, "Posture detection based on smart cushion for wheelchair users," *Sensors*, vol. 17, no. 4, pp. 1–18, 2017.
- [16] C. Ma, W. Li, R. Gravina, J. Cao, Q. Li, and G. Fortino, "Activity level assessment using a smart cushion for people with a sedentary lifestyle," *Sensors*, vol. 17, no. 10, pp. 1–19, 2017.
- [17] A. S. Sadun, J. Jalani, and J. A. Sukor, "Force Sensing Resistor (FSR): A brief overview and the low-cost sensor for active compliance control," in *Proceedings of the 1st International Workshop on Pattern Recognition*, Japan, May 2016.
- [18] FSR-408 and FSR-406, https://cdn-shop.adafruit.com/datasheets/FSR400Series_PD.pdf.
- [19] M. F. Shaikh, Z. Salcic, and K. Wang, "Analysis and selection of the force sensitive resistors for gait characterization," in *Proceedings of the 6th Int. Conf. on Automation, Robotics and Applications*, pp. 370–375, 2015.
- [20] V. Vujović and M. Maksimović, "Raspberry Pi as a wireless sensor node: performances and constraints," in *Proceedings of the 37th International Convention on Information and Communication Technology, Electronics and Microelectronics (MIPRO '14)*, pp. 1013–1018, Opatija, Croatia, May 2014.
- [21] S. Jindarat and P. Wuttidittachotti, "Smart farm monitoring using Raspberry Pi and Arduino," in *Proceedings of the 2nd International Conference on Computer, Communications, and Control Technology, I4CT 2015*, pp. 284–288, Malaysia, April 2015.
- [22] S. Rautmare and D. M. Bhalerao, "MySQL and NoSQL database comparison for IoT application," in *Proceedings of the 2016 IEEE International Conference on Advances in Computer Applications, ICACA 2016*, pp. 235–238, India.
- [23] Size Korea, Korean Agency for Technology and Standards (KATS), <https://sizekorea.kr>.

